



PEKING
UNIVERSITY

Quantum Spin Liquid in Kitaev Model with a candidate $\alpha\text{-RuCl}_3$

Group member: K.W. Sun, N.Z. Shang, Y.F. Wang, Y. Ji
孙恺伟, 尚念泽, 王一帆, 吉源

2018.12.28

What is liquid?



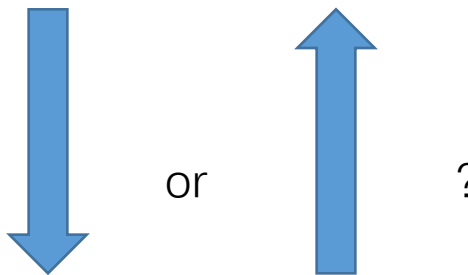
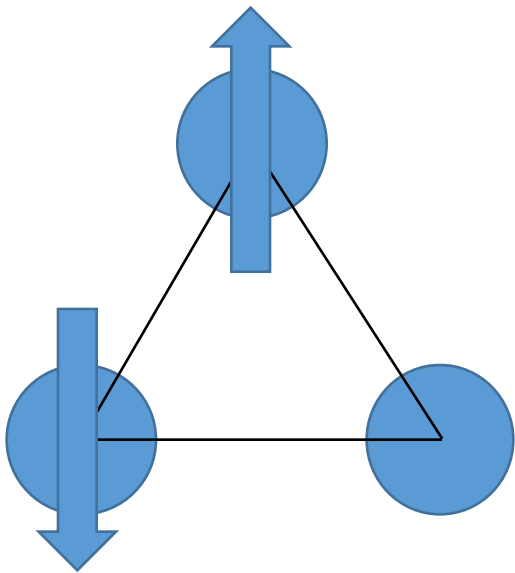
Liquid can flow. (just like a cat)

Liquid is short-range ordered, long-range disorder

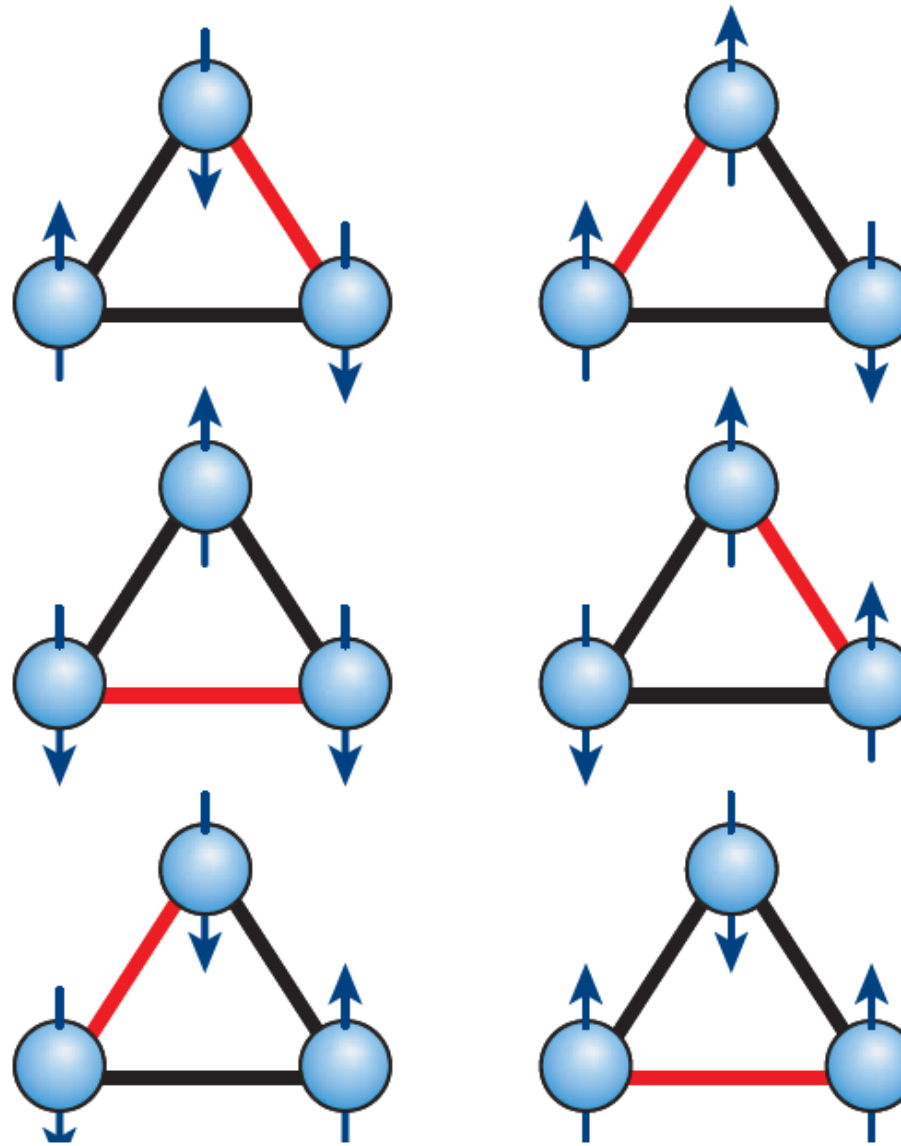


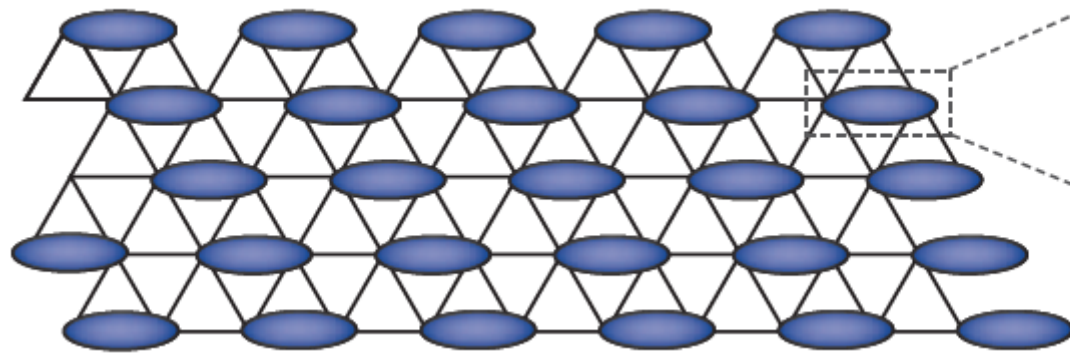
Quantum spin liquid can be found in frustrated model.

$$H = J \sum_{\langle i,j \rangle} \sigma_i^z \sigma_j^z$$

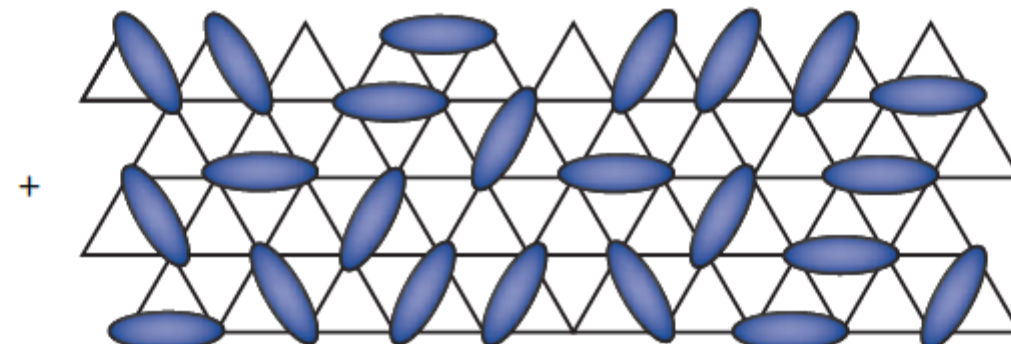
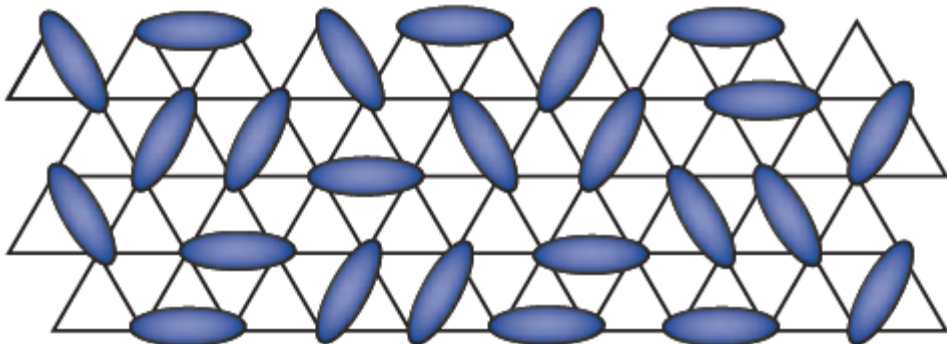


Degenerate configurations



a

$$\frac{1}{\sqrt{2}} \left(\begin{array}{c} \uparrow \\ \text{blue oval} \\ \downarrow \end{array} + \begin{array}{c} \downarrow \\ \text{blue oval} \\ \uparrow \end{array} \right)$$

b

+ ...

Kitaev Model: exactly Solvable!



Available online at www.sciencedirect.com

SCIENCE @ DIRECT®

Annals of Physics 321 (2006) 2–111

**ANNALS
of
PHYSICS**

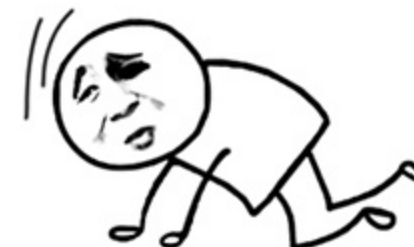
www.elsevier.com/locate/aop

Anyons in an exactly solved model and beyond

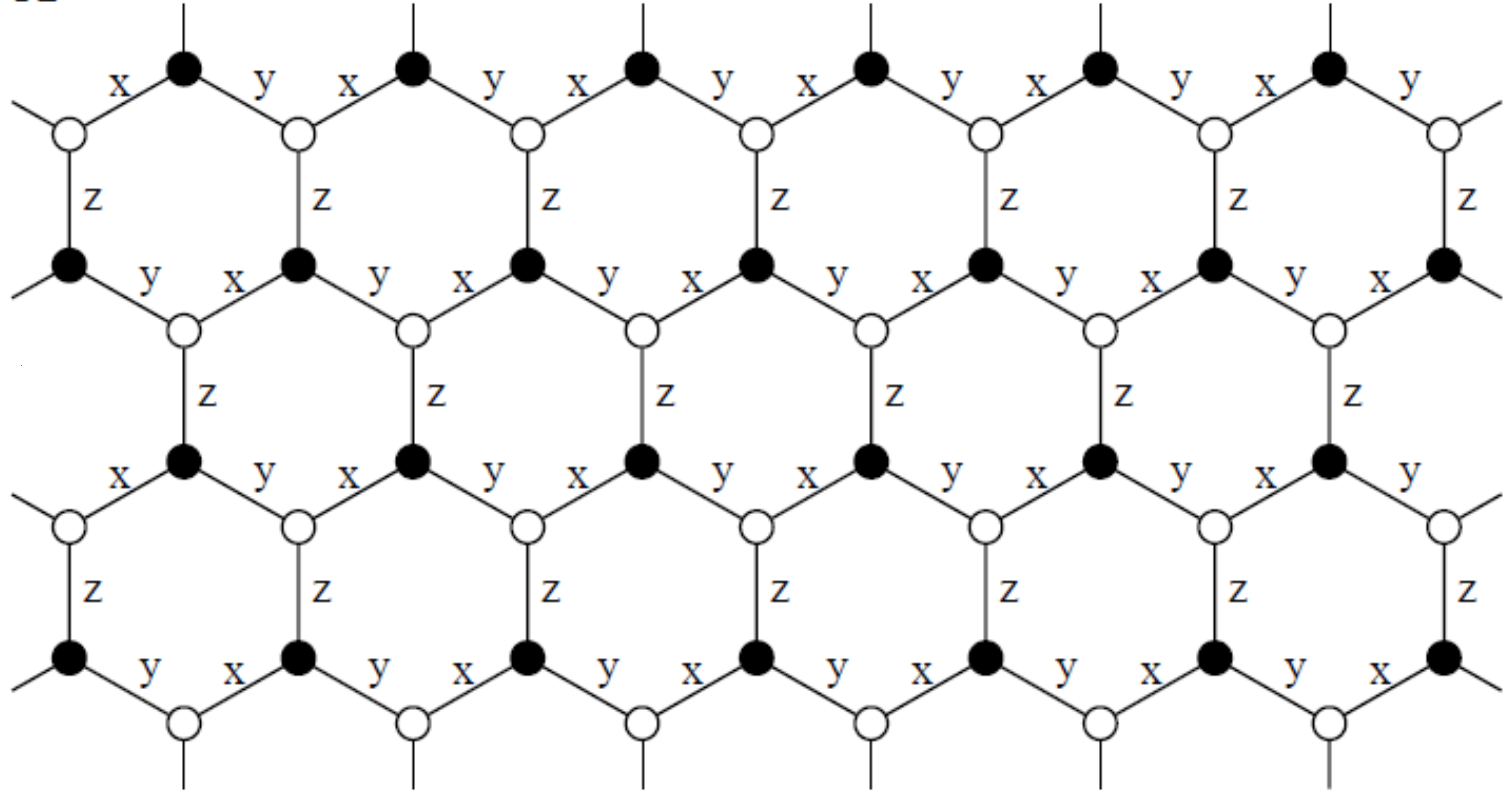
Alexei Kitaev *

California Institute of Technology, Pasadena, CA 91125, USA

Received 21 October 2005; accepted 25 October 2005



膜拜大佬

A

$$H = -J_x \sum_{x\text{-links}} \sigma_j^x \sigma_k^x - J_y \sum_{y\text{-links}} \sigma_j^y \sigma_k^y - J_z \sum_{z\text{-links}} \sigma_j^z \sigma_k^z,$$

We use Majorana Fermions decomposition to solve this problem

$$c_{2k-1} = a_k^\dagger + a_k$$

$$c_{2k} = i(a_k^\dagger - a_k)$$

Indeed, we have

$$c = c^\dagger$$

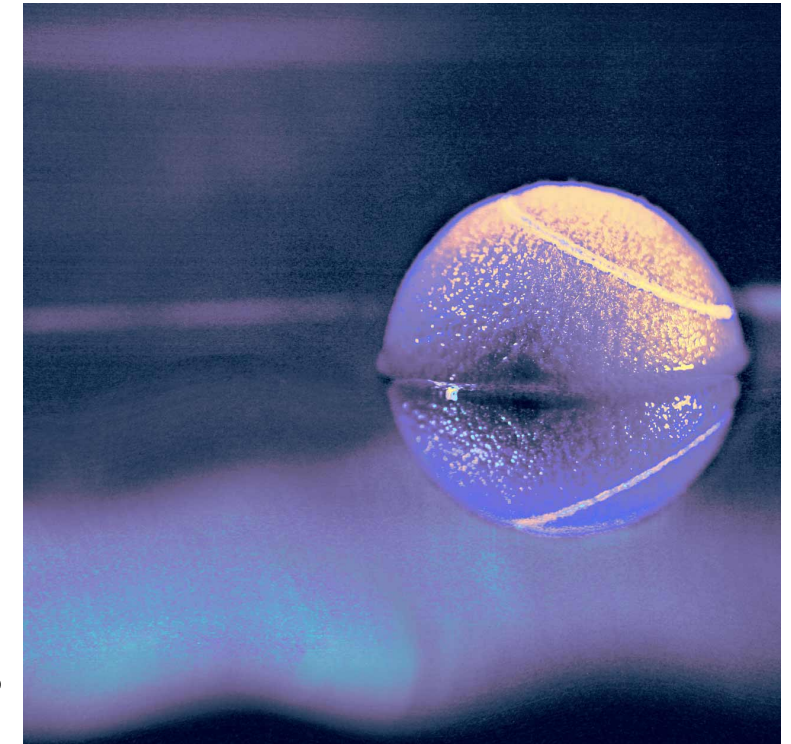
$$[c_i, c_j] = 2\delta_{ij}$$

Decompose Pauli operators into Majorana fermions

$$\sigma_i^x = i b_i^x c_i$$

$$\sigma_i^y = i b_i^y c_i$$

$$\sigma_i^z = i b_i^z c_i$$



Well, things are not so easy

On each site, **two states** with spin representation $|\uparrow\rangle$ and $|\downarrow\rangle$

Four Majorana fermions correspond to two complex fermions: **four states!**

$$c_{2k-1} = a_k^\dagger + a_k$$

$$c_{2k} = i(a_k^\dagger - a_k)$$

$$\sigma_i^x = i b_i^x c_i$$

$$\sigma_i^y = i b_i^y c_i$$

$$\sigma_i^z = i b_i^z c_i$$



We found: *Do we use Lagrangian multiplier method to treat this constrain?*

$$\sigma_i^x \sigma_i^y \sigma_i^z = i$$

On the other hand

$$\sigma_i^x \sigma_i^y \sigma_i^z = (ib_i^x c_i) (ib_i^y c_i) (ib_i^z c_i) = ib_i^x b_i^y b_i^z c_i$$

Constrain:

$$D_i \equiv b_i^x b_i^y b_i^z c_i = 1$$

Without this constrain,
Di can also be -1, not physical!



Luckily, we have

$$[D_i, H] = 0$$

We can just forget the constrain
and work with the Majorana Hamiltonian!
After this, project results to physical region using

$$P = \prod_j \frac{1 + D_j}{2}$$



Now, let's solve the Hamiltonian (with Majorana representation)!

Define:

$$u_{jk} = \begin{cases} ib_j^x b_k^x, x-links & u_{jk} = \pm 1 \\ ib_j^y b_k^y, y-links \\ ib_j^z b_k^z, z-links & [u_{jk}, H] = 0 \end{cases}$$

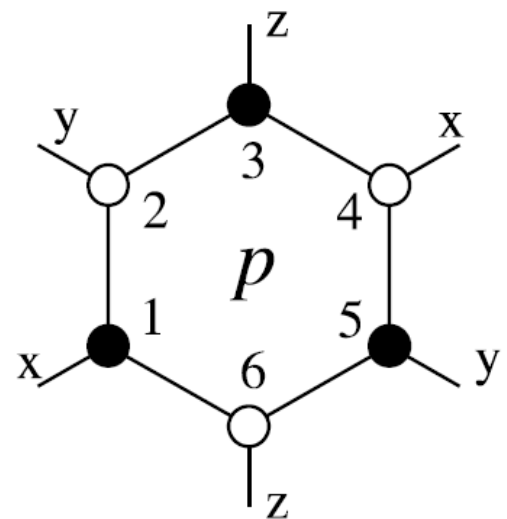
$$H = \sum_{<jk>} iJ_\alpha u_{jk} c_j c_k$$

Now we can handle this Hamiltonian with specific u-configuration, which is **quadratic!**

Lattice plaquette operator

$$W_p = u_{12} u_{23} u_{34} u_{45} u_{56} u_{61}$$

$$[W_p, H] = 0 \quad W_p = \pm 1$$



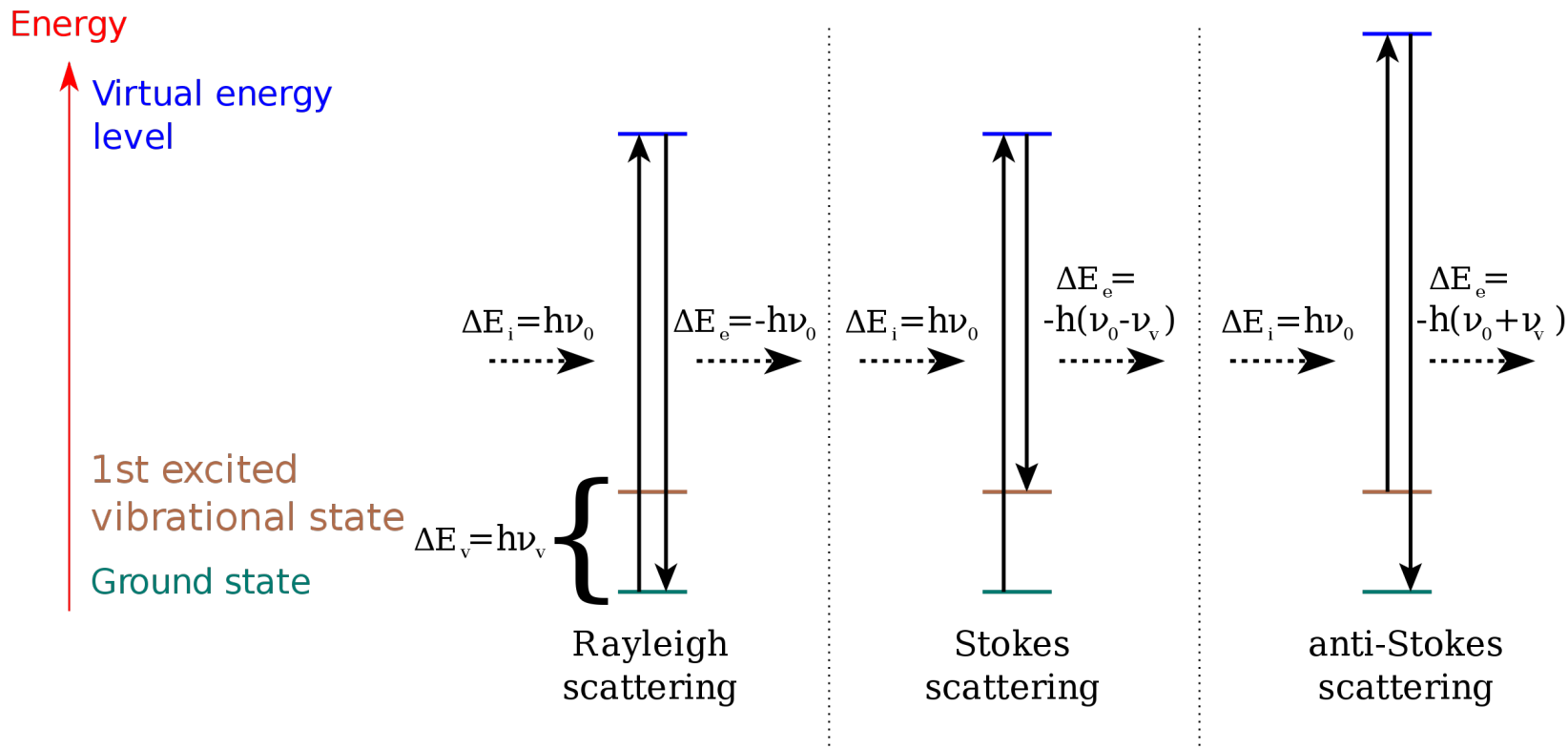
Numerical results show:

1. Ground states correspond to $W_p=1$
2. No long-range magnetic order!



Raman scattering spectroscopy

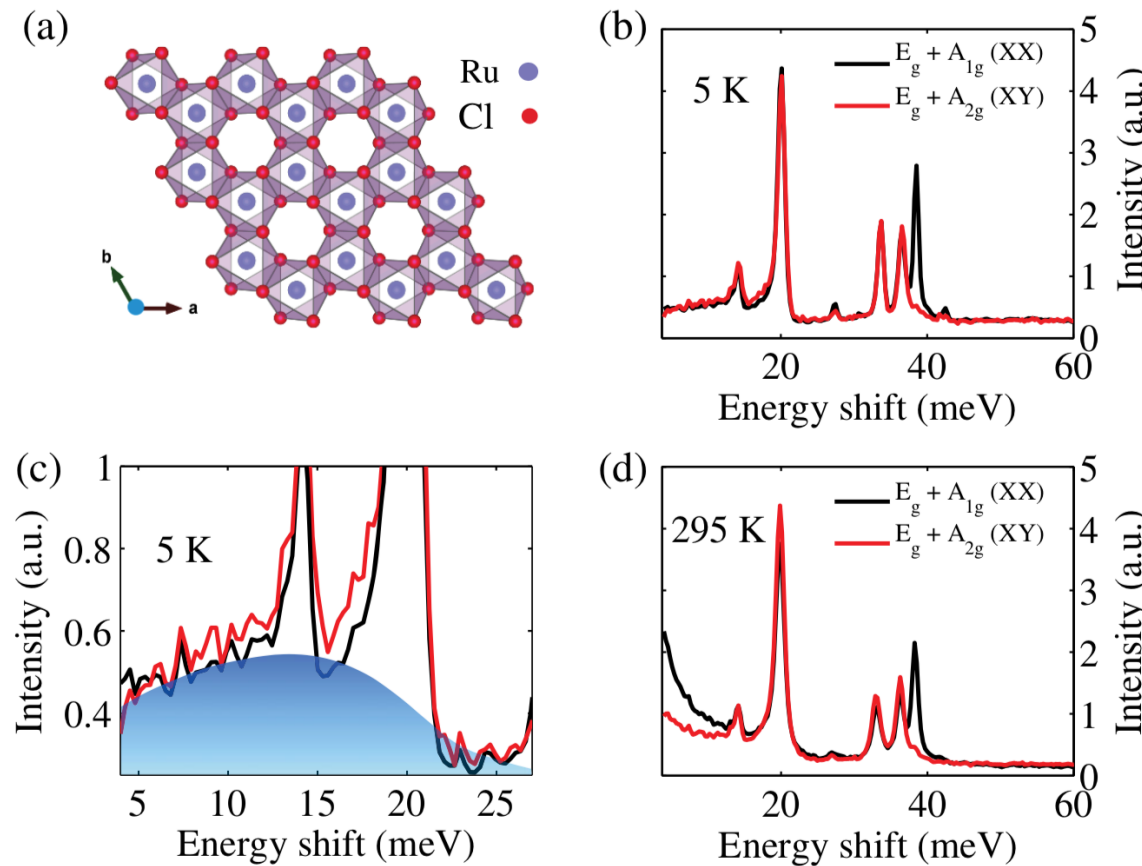
The Mechanism of Rayleigh and Raman Scattering



The energy states which the incident photon interacting with can be phonons, electrons, magnons etc.

In our case, it is declared to be that lattice spin states are responsible for the wanted Raman spectrum.

Structure and polarized Raman response of α -RuCl₃.

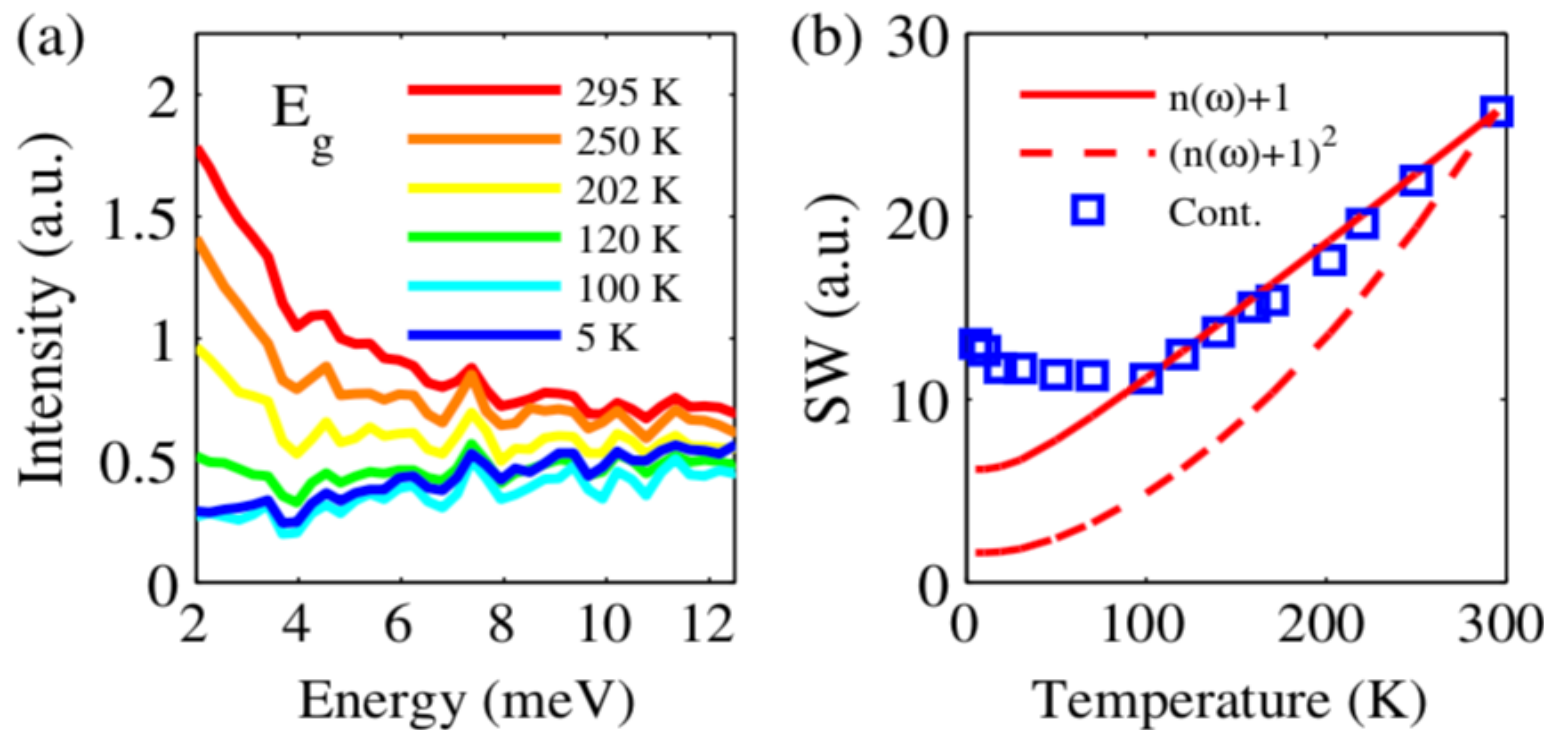


$$f(\omega) = \frac{I_s}{q^2 - 1} \frac{(q + \epsilon^2)}{1 + \epsilon^2}.$$

Due to the broad line shape and low energy, we attribute the continuum to magnetic scattering

The Fano line shape of the 20 meV phonon demonstrates that the continuum extends to at least 20–25 meV.

Magnetic scattering in RuCl₃ and temperature dependence

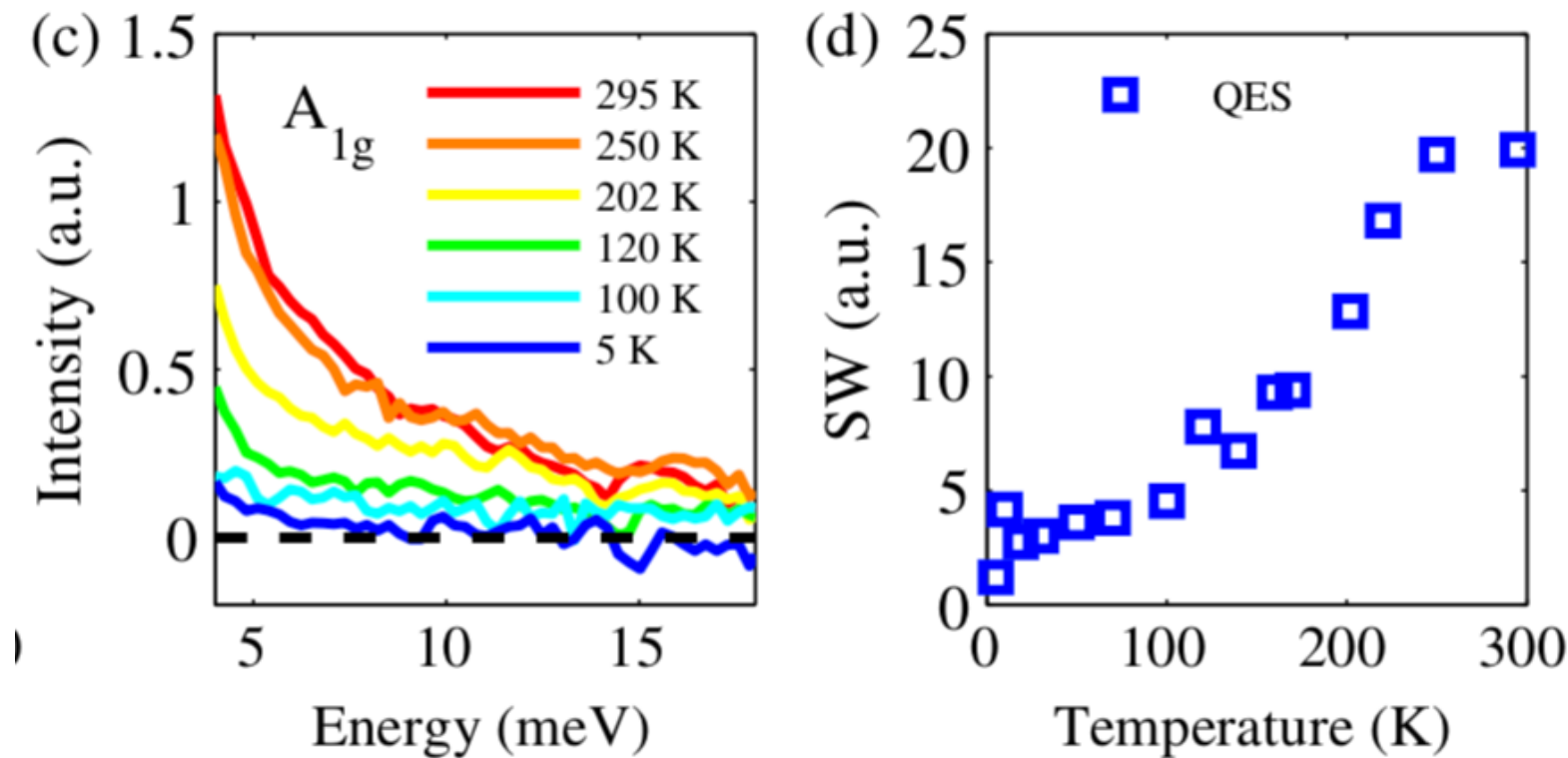


the intensity of the Eg continuum decreases as temperature is reduced to 100 K before increasing.

The change in the magnetic scattering near 100 K is consistent with the onset of in-plane spin correlation.

persistence of magnetic scattering far above T_N is a signature of frustrated, low-dimensional magnetism.

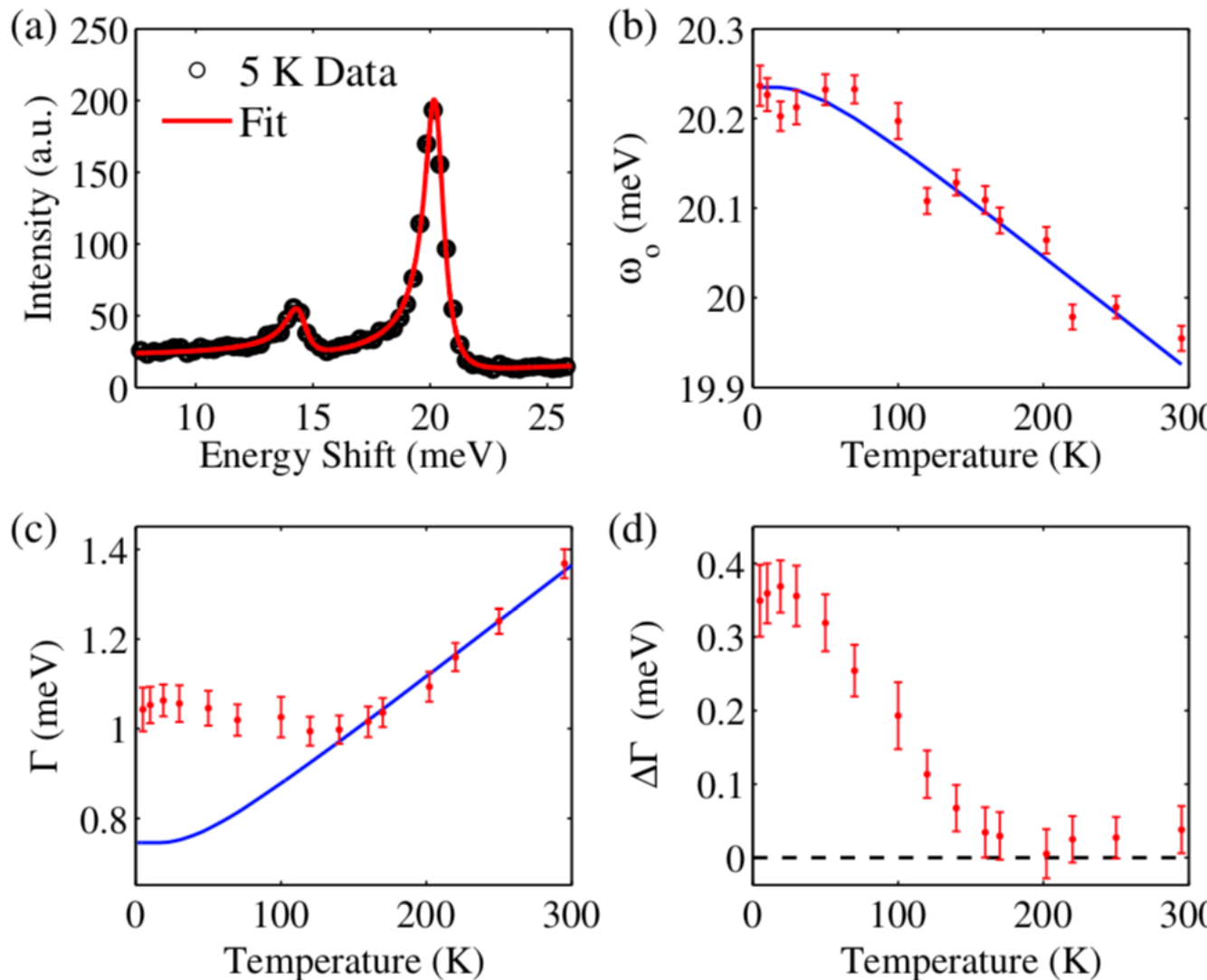
Magnetic scattering in RuCl₃ and temperature dependence



A_{1g} quasielastic scattering (QES) decreases in intensity as temperature is reduced

The change in the magnetic scattering near 100 K is consistent with the onset of in-plane spin correlation. Persistence of magnetic scattering far above T_N is a signature of frustrated, low-dimensional magnetism.

Spin-phonon coupling in α -RuCl₃ —Evidence for unusual magnetic excitations



The low-energy data are well-described by the Fano form and indicate a coupling between the magnetic continuum and the lattice.

$$\Gamma(T) = \Gamma_o + A[1 + 2n(\omega_o/2)]$$

$$\omega(T) = \omega_o - B[1 + 2n(\omega_o/2)]$$

This coupling is also apparent in the temperature dependence of Γ , which shows an anomaly near 140 K.

- revealing a continuum of scattering that is not readily explained by conventional 2M scattering or structural disorder
- experimental results appear consistent with the notion that α -RuCl₃ hosts unusual magnetic excitations, possibly driven by proximity to a Kitaev QSL state.
- More solid experimental proof required, such as neutron scattering, NMR.

nuclear-magnetic-resonance
measurements

Nuclear-Magnetic-Resonance measurements



Kurt Wüthrich,
1938.
2002年
诺贝尔化学奖



Sir Peter Mansfield,
1933.
1991年
诺贝尔医学奖



ENC Boston 1995

Richard R. Ernst,
1933.
1991年
诺贝尔化学奖

Edward M. Purcell,
1912—1997.
1952年
诺贝尔物理学奖



Felix Bloch,
1905—1983.
1952年
诺贝尔物理学奖



Paul Lauterbur,
1929.
2003年
诺贝尔医学奖

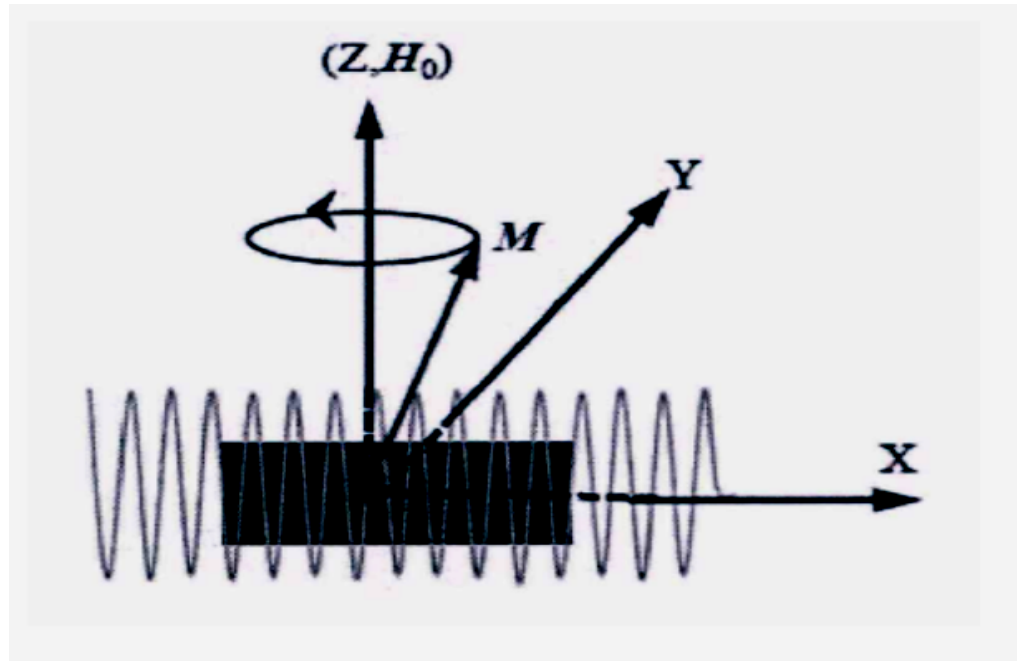
📎 F.Bloch and E.M. Purcell in 1940's, **CW NMR**, Nuclei Magnetic Resonance in Solids and Liquids with RF field(1952 Nobel prize in Physics)

📎 R.R. Ernst in 1960's, **Pulse NMR**, Fourier Transform(FT) and multi dimensional NMR.(1991 Nobel prize in Chemistry)

📎 K. Wuthrich, **protein FT NMR**, (2002 Nobel prize in Chemistry)

📎 P.Lauterbur and S.P. Mansfield, **MRI**, (2003 Nobel prize in Physiology or Medicine)

Nuclear-Magnetic-Resonance measurements



NMR signal generation schematic

$$K = (f - f_0) / f_0 = (\gamma_n B - \gamma_n B_0) / \gamma_n B_0$$

$$K_n = A_{orb} \chi_{orb} + A_{hf} \chi_s(T)$$

Bloch description:

$$dM_x / dt = \gamma(M \times B)_x - M_x / T_2$$

$$dM_y / dt = \gamma(M \times B)_y - M_y / T_2$$

$$dM_z / dt = \gamma(M \times B)_z - (M_\infty - M_z) / T_1$$

$$\downarrow \quad t=0, \quad B_0 = (0, 0, B_z)$$

Relaxation Equation of longitudinal magnetic moment(z-):

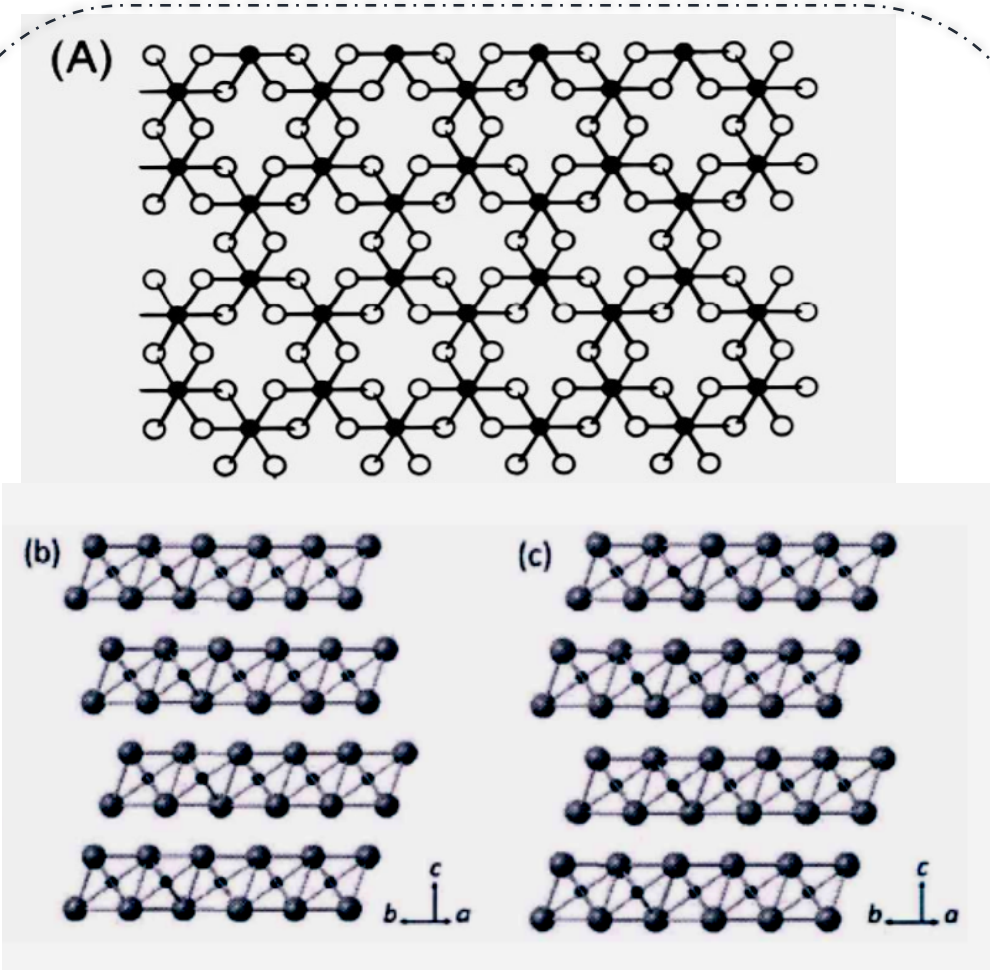
$$M_z(t) = (M_\infty - M_z(0))e^{-t/T_1}$$

Relaxation Equation of lateral magnetic moment(xy):

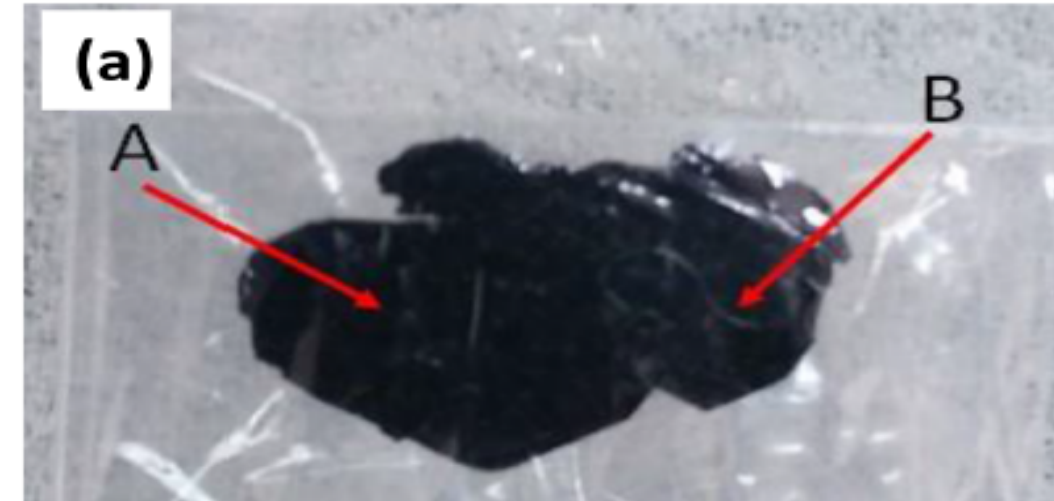
$$M_\perp(t) = M_\perp(0)e^{-t/T_2}$$

The electrons around the nucleus, with orbital magnetic moments and spin magnetic moments, create additional magnetic fields that cause the Knight's displacement. The track portion usually does not change with temperature, and A_{hf} is a hyperfine coupling constant.

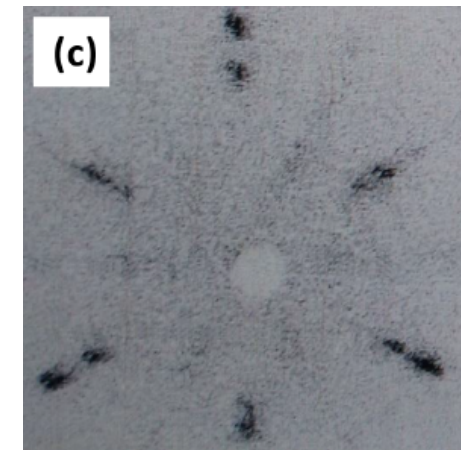
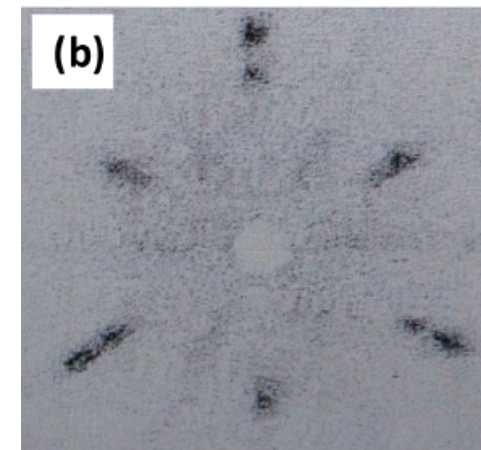
Introduction to NMR



J. Am. Chem. Soc., Vol. 122, No. 28, 2000



(a) The single crystal sample of α -RuCl₃



(b) Von Laue diffraction pattern measured at spot A on the sample.
(c) Von Laue diffraction pattern measured at spot B on the sample.

Magnetization & Low-T specific heat & ^{35}Cl NMR spectra

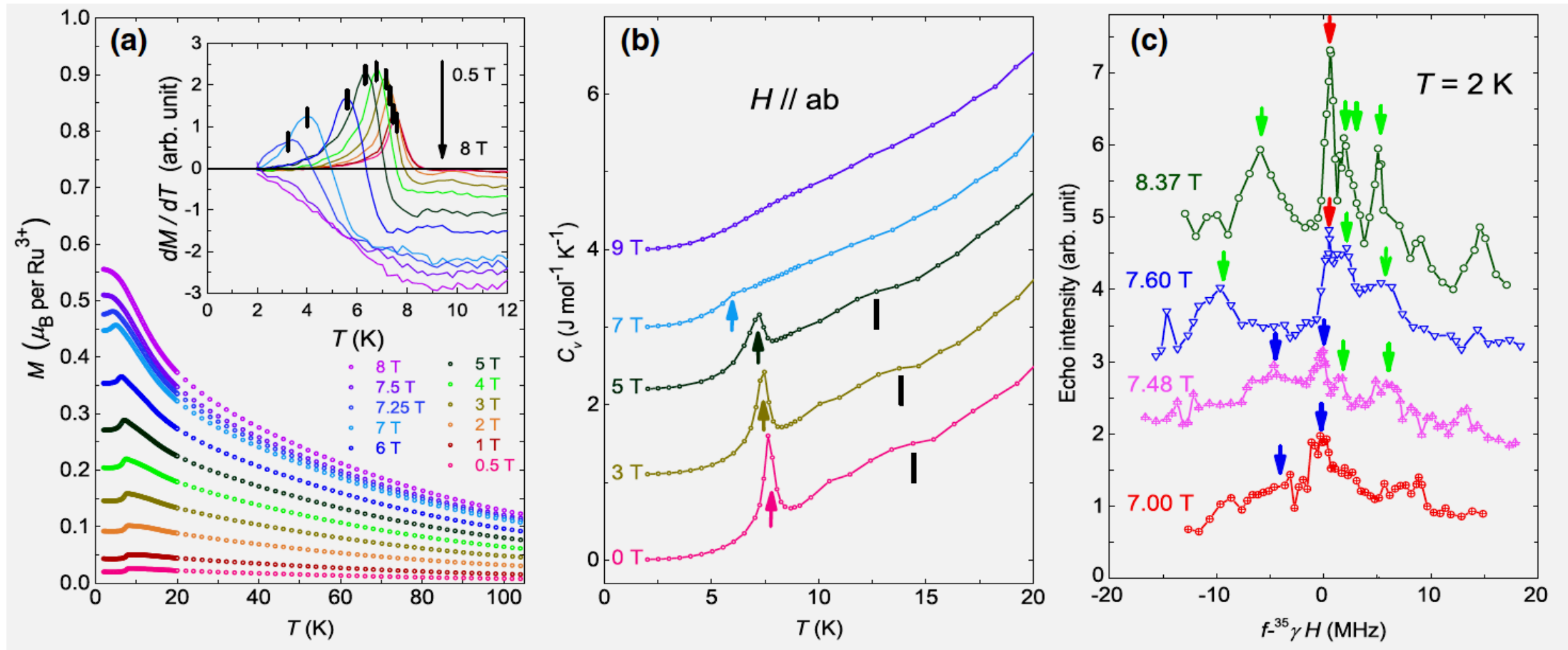


FIG. 2. Magnetic transition with field applied in the ab plane. (a) Magnetization, $M\delta T\mu$. Inset: $dM=dT$; vertical lines mark the peaks, which show TN for fields up to 7.25 T. (b) Low-T specific heat, C_v . Data are offset for clarity. The transition for regions with ABC (AB) layer stacking is marked by the arrows (vertical lines). (c) ^{35}Cl NMR spectra at fields close to 7.5 T, shown at $T= 2 \text{ K}$.

^{35}Cl NMR spectra and Knight shift

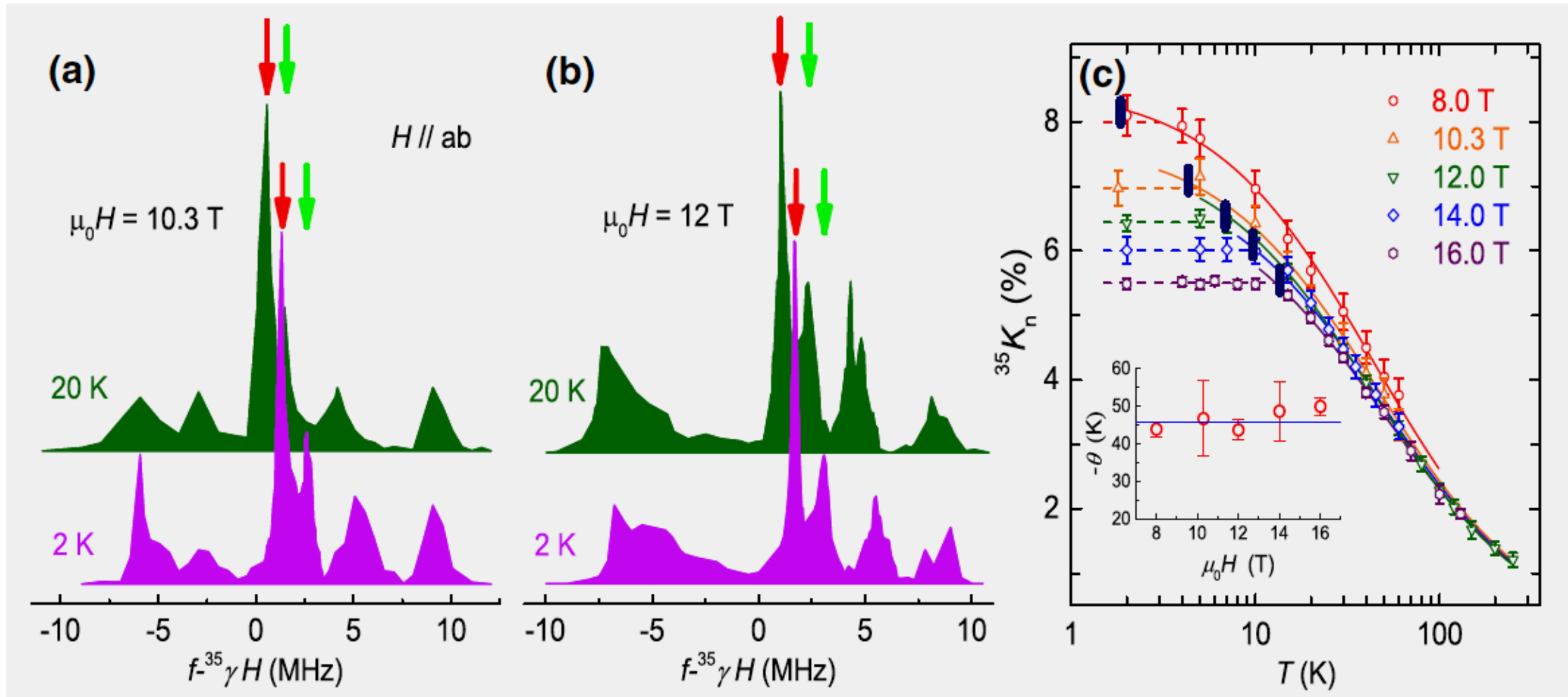


FIG. 3. ^{35}Cl NMR spectra and Knight shift for in-plane fields. ^{35}Cl spectra measured at (a) 10.3 and (b) 12 T, shown for $T = 2$ and 20 K. (c) NMR Knight shift, $^{35}K_n(T)$, measured at the central peak and shown for different field values.

NMR spin-lattice relaxation

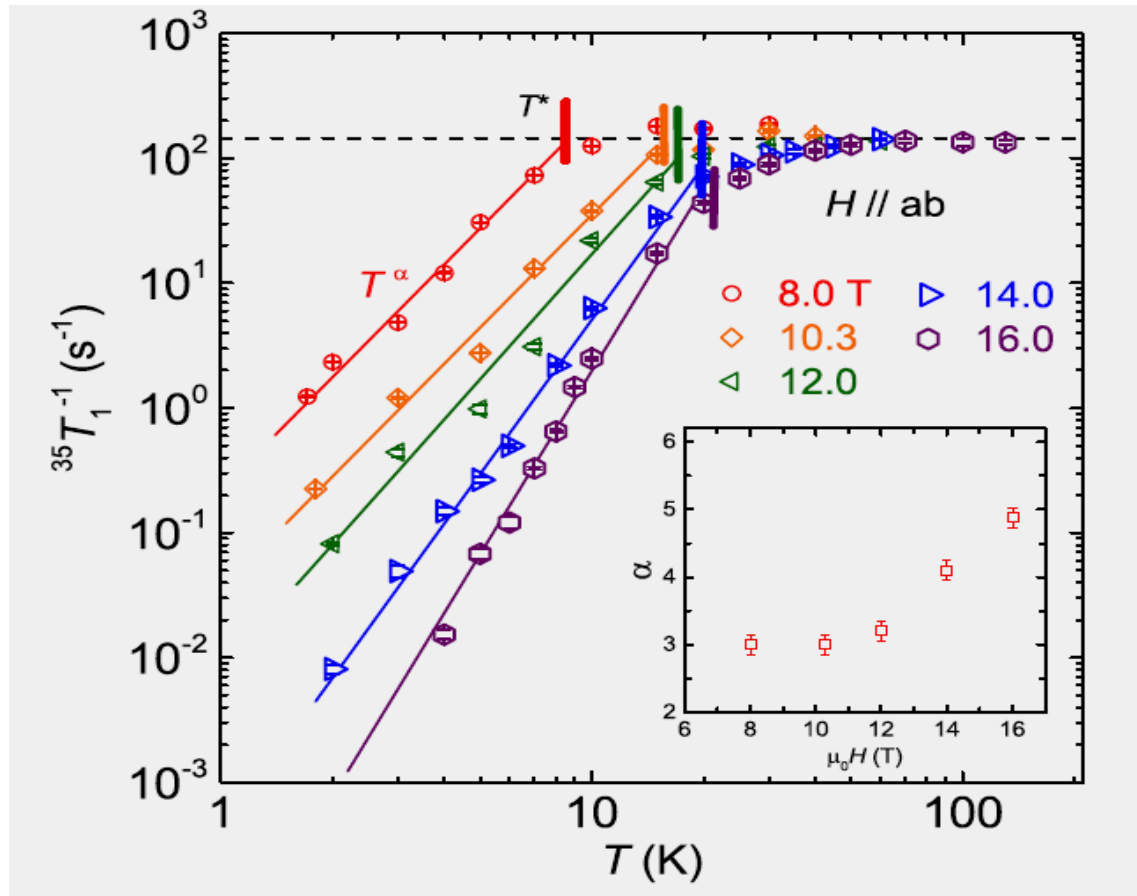


FIG. 4. NMR spin-lattice relaxation rates

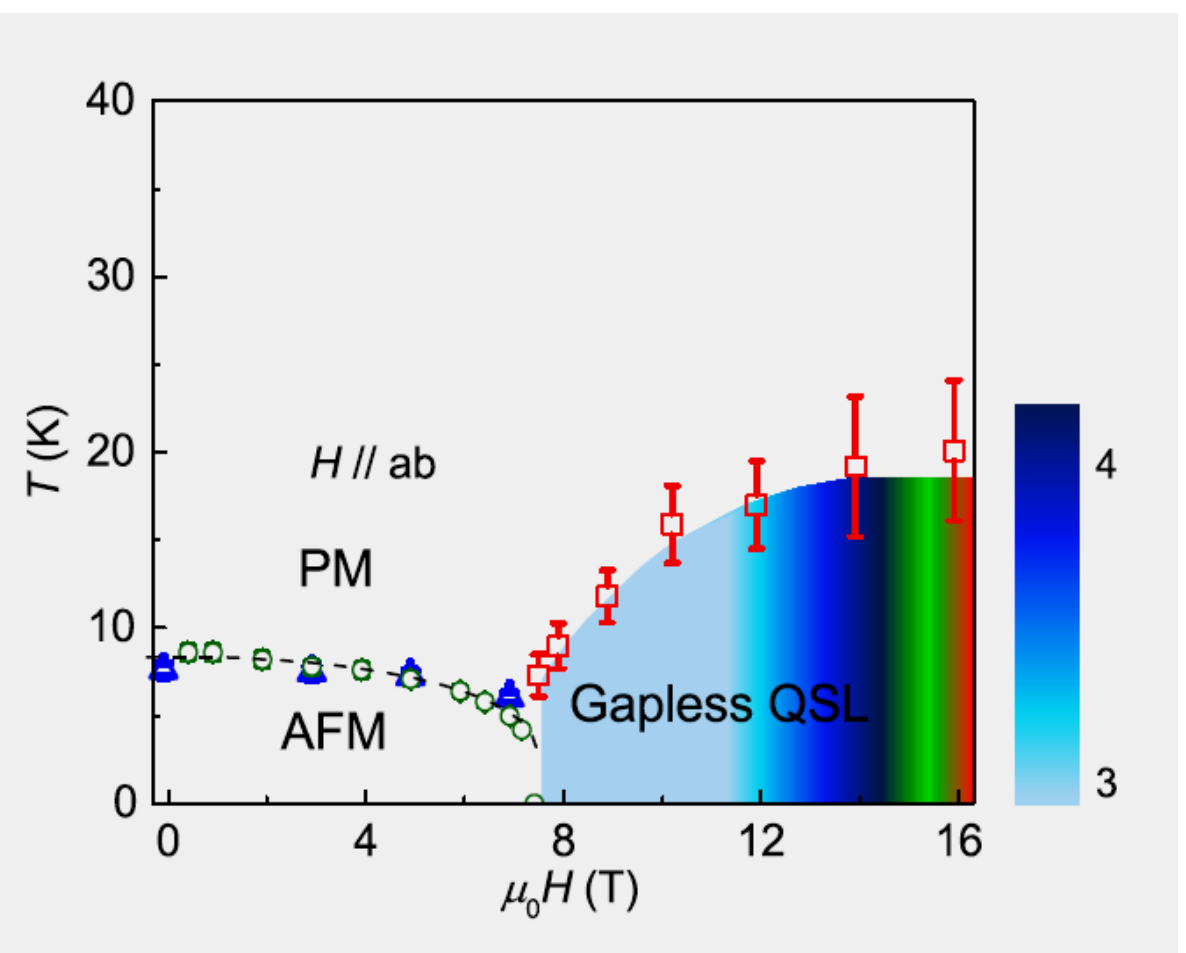
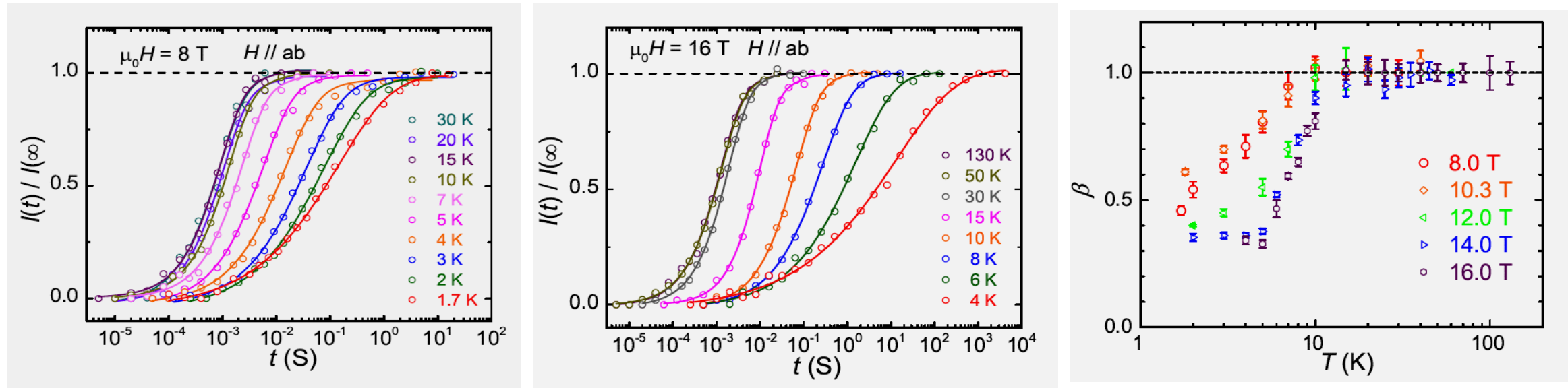


FIG. 1. Magnetic phase diagram of α -RuCl₃ with field applied in the ab plane.

Explanation



8T和16T下用核磁共振自旋-恢复方法对不同温度进行测量，并拟合。

ab面内，不同磁场下拉伸因子关于温度的函数

$$I(t) = I(\infty)[1 - a[0.1 \exp(-(t/T_1)^\beta) + 0.9 \exp(-(6t/T_1)^\beta)]]$$

- 20K以上， $\beta=1$ ，为顺磁相，表明高质量样品态
- T^* 以下，进入QSL区， β 下降，表明自旋动力学对无序的强烈敏感性。



观测到的QSL相可能不是内在属性，是无序性的结果。

neutron scattering

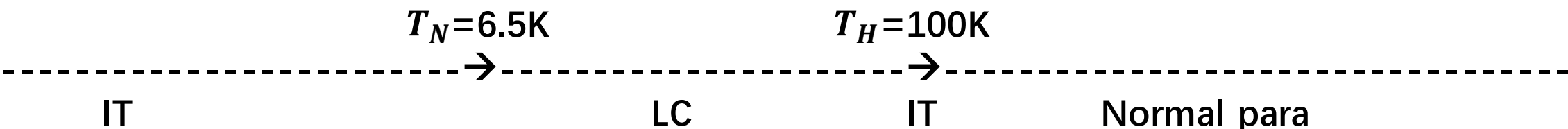
The elementary excitations of a Kitaev QSL are **localized and itinerant Majorana fermions**

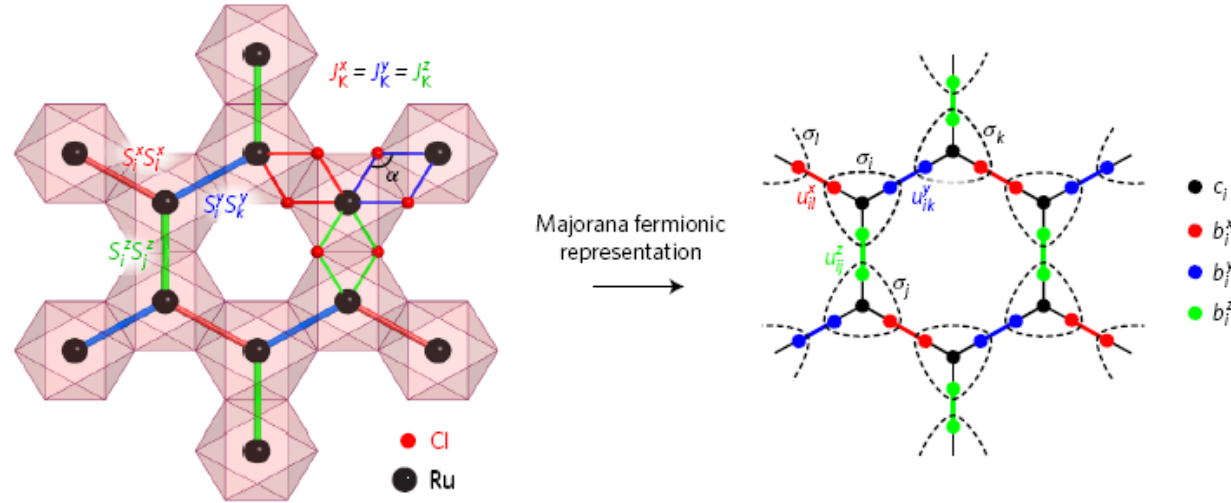
Why choose vdW alpha-RuCl₃:

Recently, significant advances in the synthesis of high-quality RuCl₃ crystals have been achieved. These crystals are almost free from stacking faults(层叠错位).

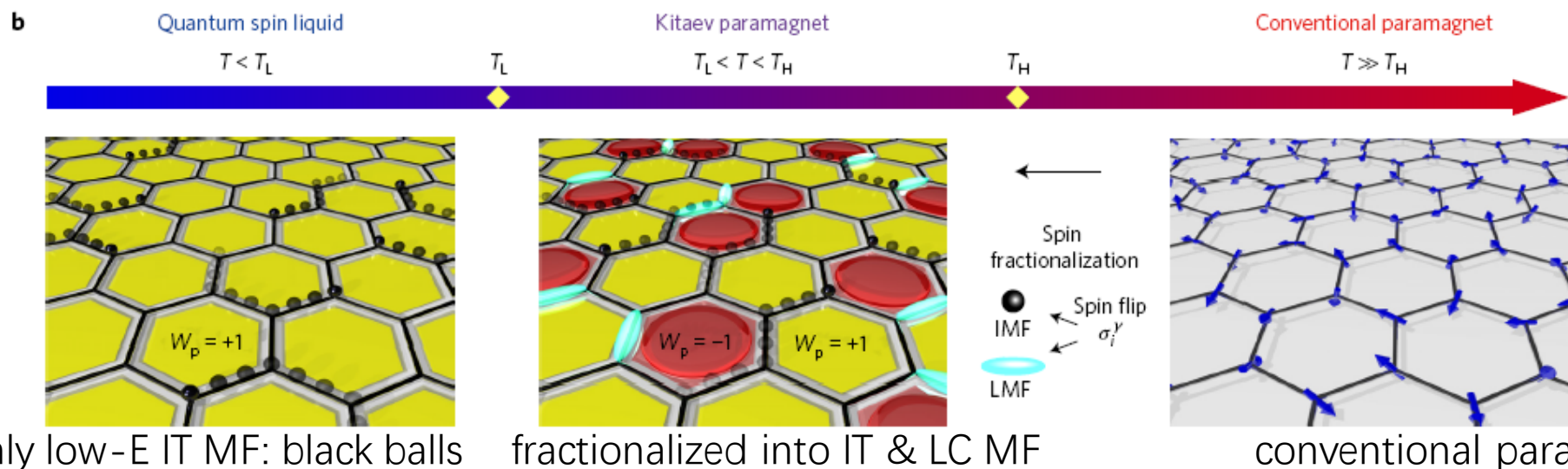
Importantly, this high-symmetry structure renders isotropic Kitaev interactions with a **94 degree Ru-Cl-Ru** contribution becomes bond angle **maximizing the Kitaev interaction, and the Heisenberg minimal.**

Advance in QMC & CDMFT: It is predicted that thermally fluctuating quantum spins are successively fractionalized into itinerant and localized Majorana fermions(IT, LC for short)





Pauli spin operator: $\sigma_i^\gamma = i b_i^\gamma c_i$, where b_i^γ denotes localized MF; c_i denotes itinerant MF in extended Hilbert space



Thermodynamic signatures of spin fractionalization

Below 140K, deviates from Curie-Weiss curve → Onset of short-range spin correlation

Kink @6.5K in χ and C_M → onset of zigzag-type AFM order → Neel T

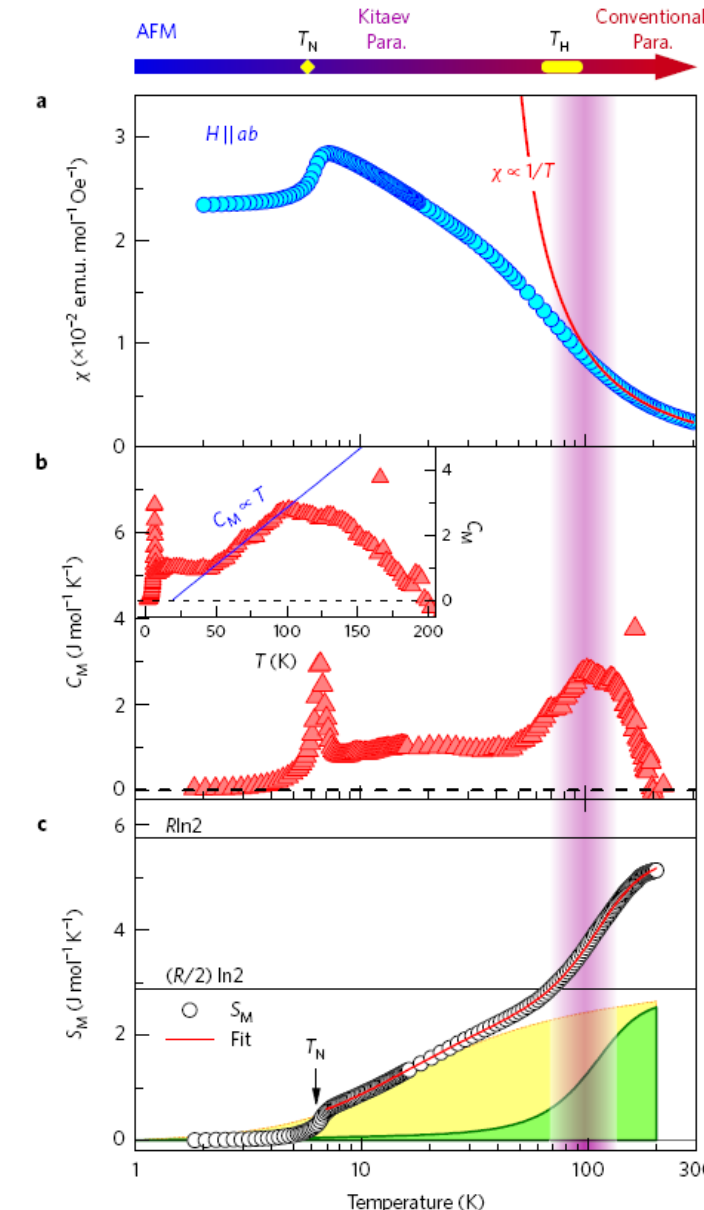
$$C_M = C_p(\text{total specific heat}) - C_{lattice}$$

Two maximum in C_M , T_L & T_H , as predicted in theory, can be ascribed to itinerant and localized MF. The linearity of inset reflects metallic behavior of itinerant MF

$$\text{Magnetic entropy: } S_M = \int C_M/T dT$$

Agree well with Schottky-like func (sum of low-T and high-T)

$$S_M = \sum_{a=L,H} \frac{\rho_a/2}{1 + \exp \left[\left(\frac{\beta_a + \gamma_a T_a/T}{1 + T_a/T} \right) \ln \left(\frac{T_a}{T} \right) \right]} ,$$

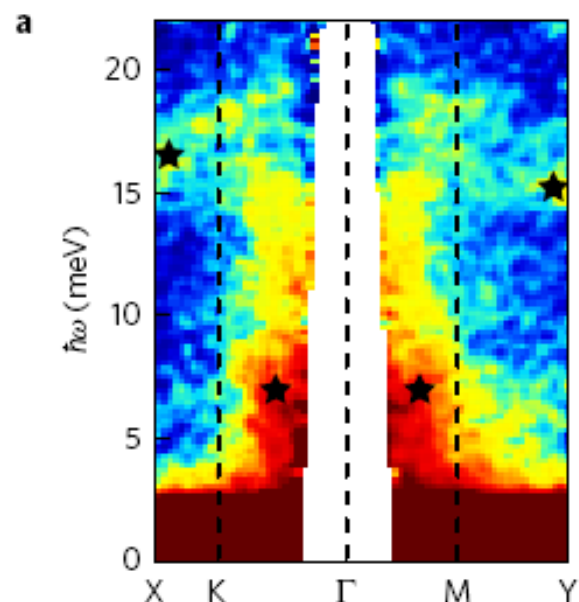


INS energy diff @ $10K > T_N$

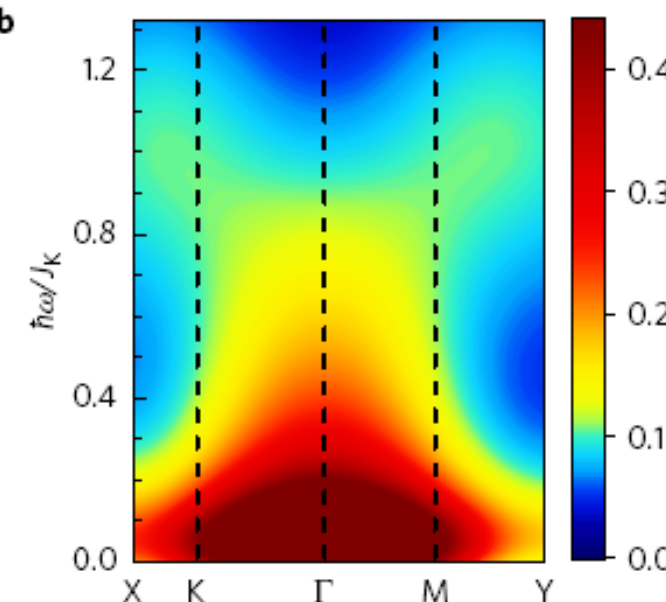
Incoming neutron energy: 31meV

At low T , $\delta_{tot}(Q, \omega) \sim \delta_{mag}(Q, \omega)$

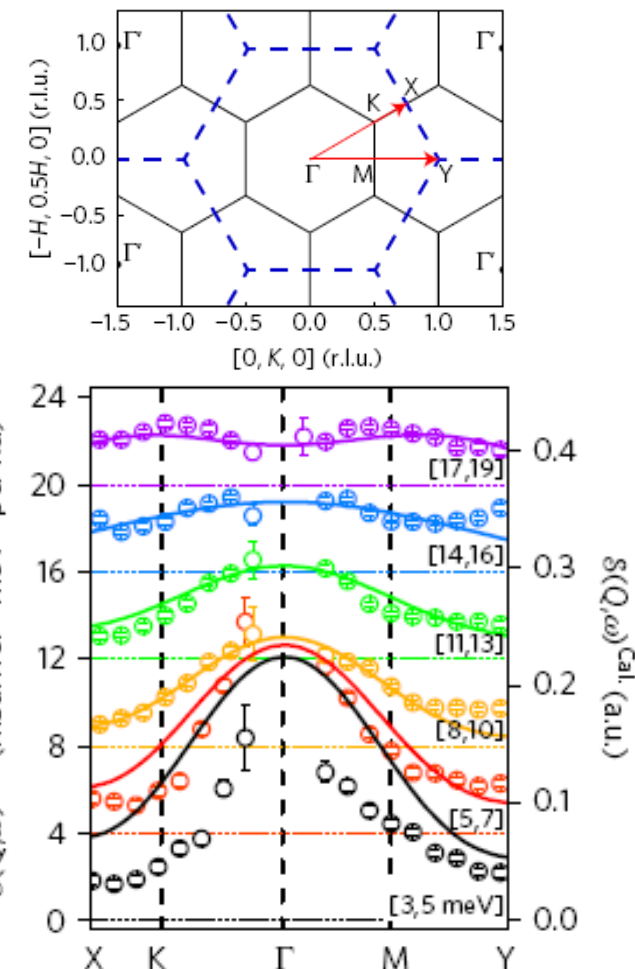
$Q\text{-}k$ momentum transfer $\hbar\omega$ – *energy transferred E*



漏斗状 around Γ
Strong excitation at low E
Y-shaped excitation at high E
star: phonon

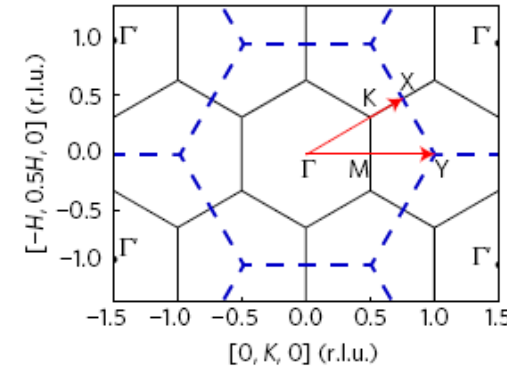
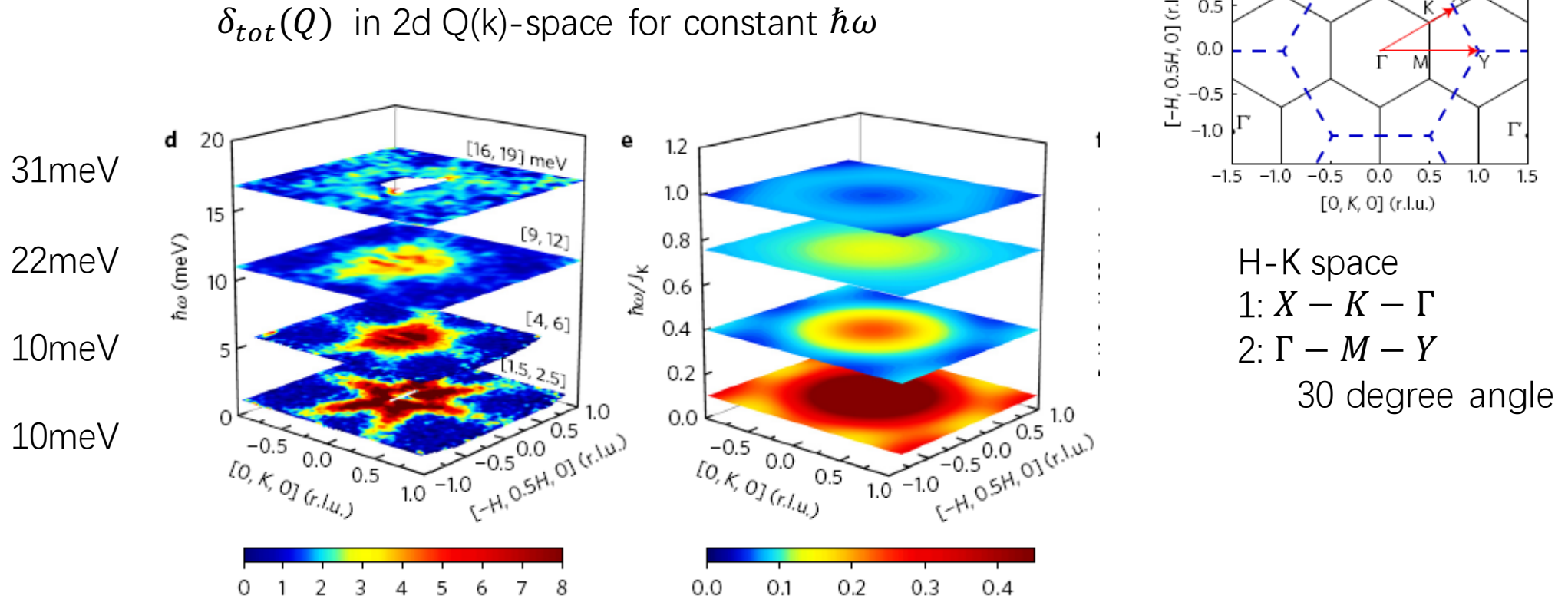


Simulated using FM Kitaev model
 $J_K = -16.5\text{meV}$
 Low E: quasielastic response
 High E: dispersive itinerant Majorana fermions



Solid: pure Kiteav

Const-E cut in hk plane

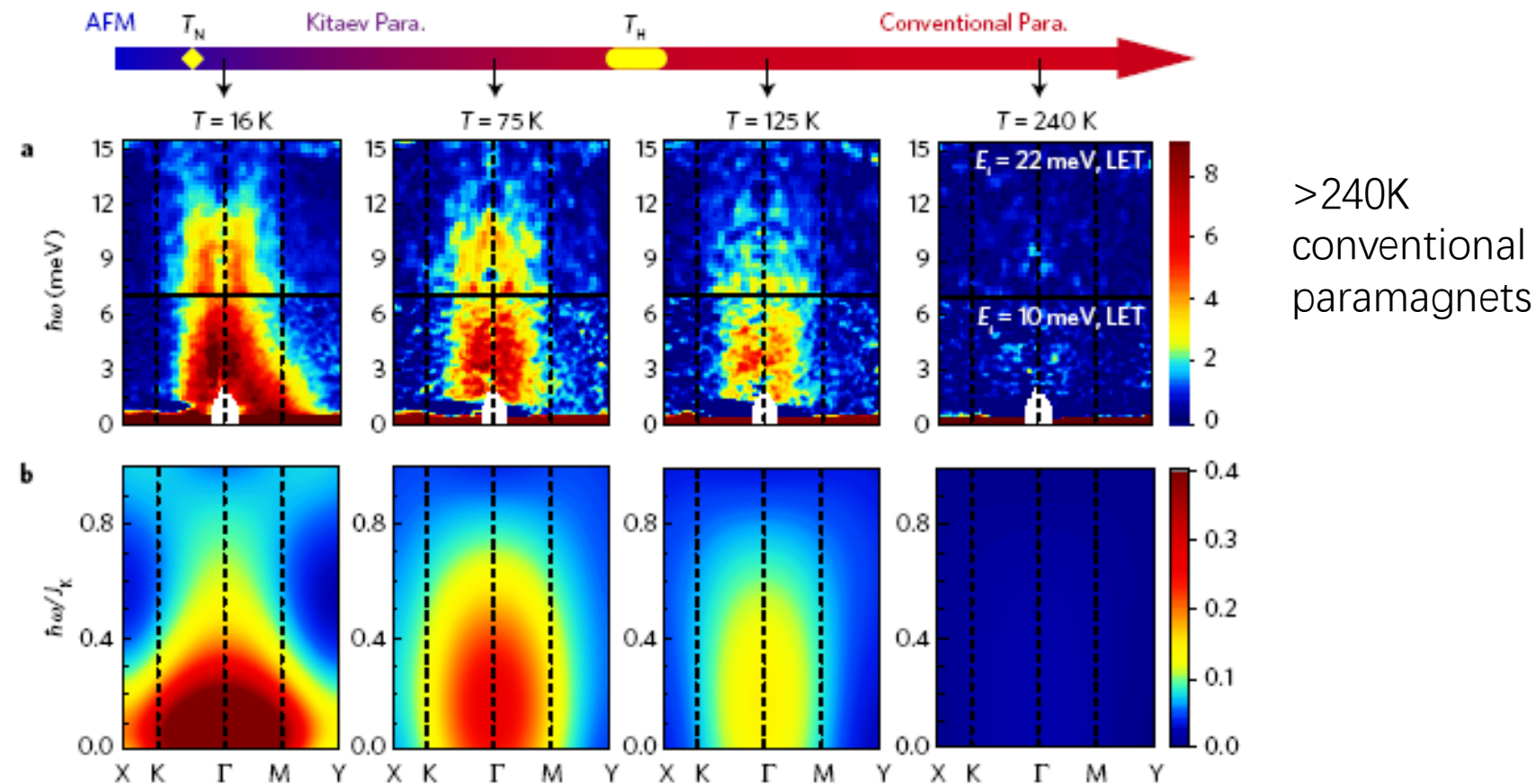


H-K space
1: $X - K - \Gamma$
2: $\Gamma - M - Y$
30 degree angle

*Out of pure Kitaev model 在低能情况下 这些作用变大(AFM $< T_N$)
The hexagon at low T is not reproduced—related to 2nd nearest-neighbor Kitaev interaction and/or symmetric anisotropy exchange interactions

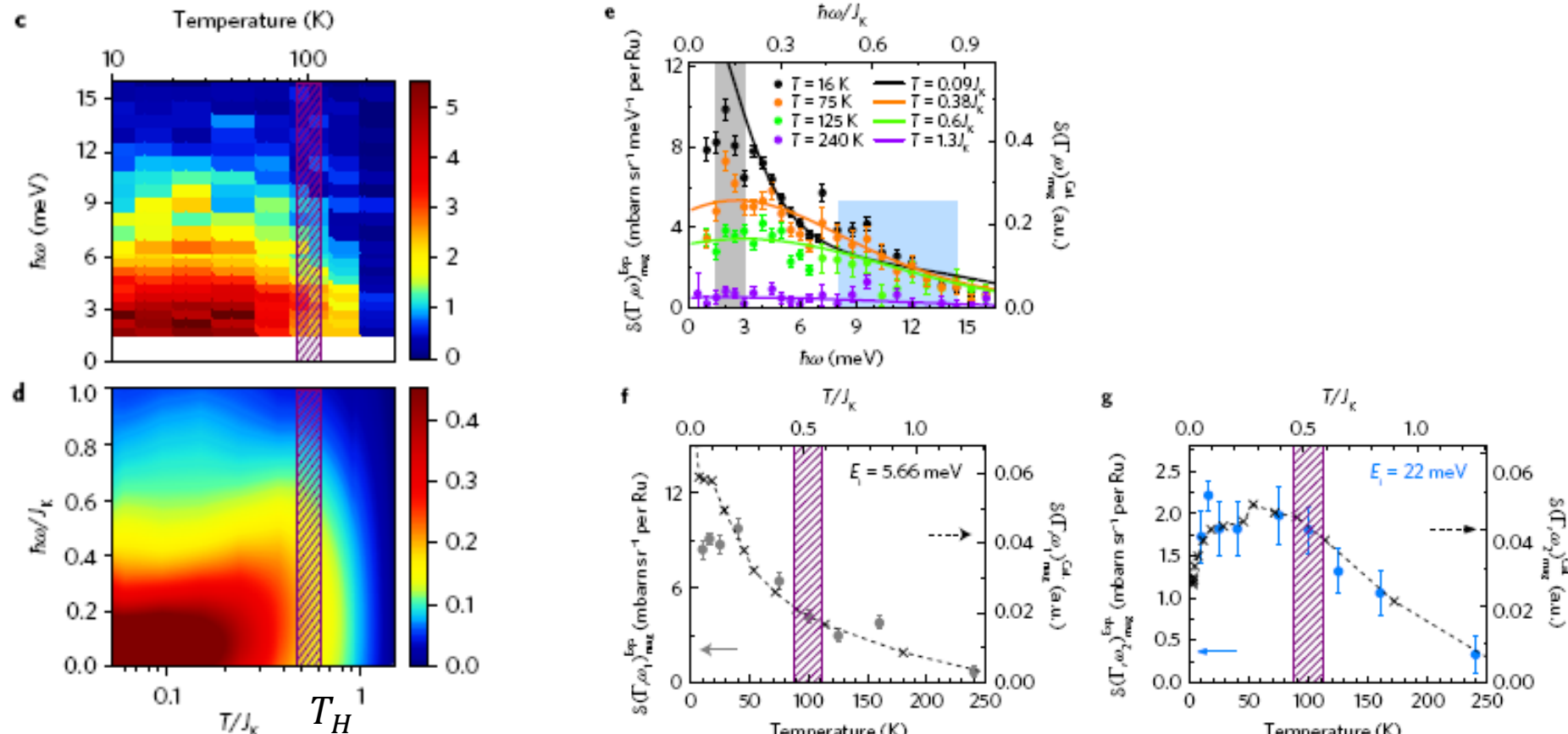
Evolution of localized and itinerant Majorana fermions with T

Kitaev paramagnetic phase
Low-E Localized Majorana fermions fades;
high-E itinerant Majorana fermions is almost maintained



Localized and itinerant MF: $\delta_{mag}(\Gamma, \omega)$ vs. (E , T)

$\delta_{mag}(\Gamma, \omega)$ is obtained by integrating $\delta_{mag}(Q, \omega)$ within $|H| < 0.12$, $|K| < 0.2$ in H-K plane



Localized MF(LMF): low E , low T
Itinerant MF(IMF): higher E , higher T

左图：低能激发LMF主要集中在低温区
右图：高能激发IMF延展到了较高温度

- Above T_N , well predicted by pure Kitaev model
- Below T_N , AFM mode appears and deteriorate QSL behavior
- When the temperature is higher than the energy scale related to the perturbing magnetic interactions, the two distinct Majorana fermions predicted in the Kitaev honeycomb model are unveiled.